

Multiple Different Black Box Explanations for Image Classifiers

Hana Chockler¹, David A. Kelly¹, Daniel Kroening^{2*}

¹ King’s College London, UK
hana.chockler,david.a.kelly@kcl.ac.uk

²Amazon, UK
daniel.kroening@magd.ox.ac.uk

February 15, 2024

“If one is investigating things that are not directly perceptible, and if one sees that several explanations are possible, it is reckless to make a dogmatic pronouncement concerning any single one; such a procedure is characteristic of a seer rather than a wise man.”

Diogenes

Abstract

Existing explanation tools for image classifiers usually give only a single explanation for an image’s classification. For many images, however, both humans and image classifiers accept more than one explanation for the image label. Thus, restricting the number of explanations to just one is arbitrary and severely limits the insight into the behavior of the classifier. In this paper, we describe an algorithm and a tool, MULTIREX, for computing multiple explanations of the output of a black-box image classifier for a given image. Our algorithm uses a principled approach based on causal theory. We analyse its theoretical complexity and provide experimental results showing that MULTIREX finds multiple explanations on 96% of the images in the ImageNet-mini benchmark, whereas previous work finds multiple explanations only on 11%.

1 Introduction

Neural networks (NN) are now a primary building block of most computer vision systems. The opacity of NNs creates demand for explainability techniques, which attempt to provide insight into why a particular input yields a particular

*This work was done prior to joining Amazon.

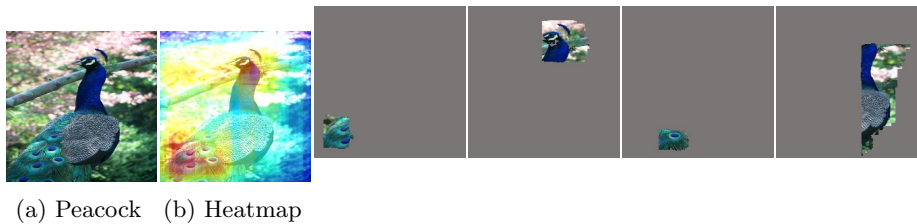


Figure 1: An example of an image ('peacock') and its maximally disjoint explanations. All explanations had 'peacock' as the top classification from the model and are not fixed to a rigid grid. The heatmap in (b) shows two distinct peaks, suggesting the presence of multiple explanations.

observed output. Beyond increasing a user's confidence in the output, and hence also their trust in the AI system, these insights help to uncover subtle classification errors that are not detectable from the output alone Chockler et al. (2021).

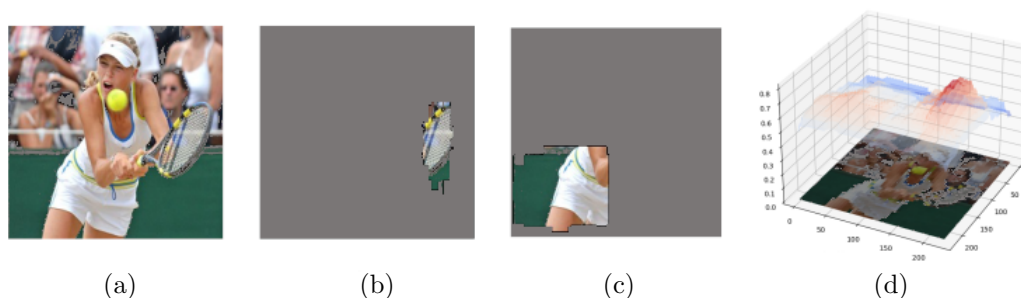


Figure 2: The image (a) is classified as 'tennis racket'. Its disjoint explanations found by MULTIREX are in (b) and (c). The first explanation is a part of a racket, and the second explanation uncovers a misclassification, as it is the player's shorts. For both (b) and (c), the top classification was 'tennis racket'. (d) is the saliency landscape. The two separate peaks in the landscape clearly indicate the presence of multiple explanations.

The most commonly used definition of an explanation is a part of the input image that is sufficient for the classifier to yield the same top label as the original image. If the top classification for the model is, say, 'peacock' (Figure 1), then we want a valid explanation to also have 'peacock' as top classification. Explanations, according to this definition, are obviously not unique. Our results show that $\approx 96\%$ of the images have multiple disjoint explanations (Table 1).

Why do we need to have multiple explanations? First of all, giving more than one explanation allows human users to choose the most suitable ones for them, hence increasing trust Hanson (2010); Miller (2019). In fact, automatically selecting just one explanation to output limits the utility of the explanation tool.

Secondly, the prevalence of multiple explanations suggests that algorithms for computing more than one explanation are essential for understanding image classifiers and uncovering subtle classification errors. The image in Figure 2 is classified by VGG19 as a tennis racket, with the first explanation indeed being a part of the racket. However, the second explanation is the player’s shorts, uncovering a misclassification. In both cases, the classification ‘racket’ is the top classification in the softmax output of the model. Yet, most existing techniques provide only one explanation, likely missing the error.

The one notable exception is SAG Shitole et al. (2021), the pioneering work in the exploration of multiple explanations for image classifiers (see Section 2 for a detailed overview). SAG uses a beam search over a 7×7 grid to discover multiple explanations. This strategy results in the search space of size 2^{49} (the number of subsets of regions of the SAG grid), and SAG attempts to solve the exponential explosion problem by randomly slashing the search space. In addition, SAG’s definition of importance, on which their explanations rely, is more permissive than the one used by most common black box tools. As we demonstrate in Section 5, if we limit SAG to our, stricter definition of explanation (‘altered SAG’ or A-SAG from now on), it fails to produce any explanations on $\approx 80\%$ of images. This is hardly surprising; as we prove in Section 3, the problem of computing multiple explanations is intractable. Specifically, we present an exponential upper bound on the number of possible explanations and demonstrate that this bound is tight.

Finally, we note that not all multiple explanations are equally valuable. Specifically, the explanations need to sufficiently differ from each other to be of value to the human user. There is a growing body of work analysing the human perception of images Fan et al. (2020); van Dyck et al. (2021) and how this differs from what NNs do. Roughly speaking, humans do not detect small differences. In particular, there is little sense in checking the effect of changing one pixel or any small number of pixels, as a new explanation would be either indistinguishable to the human eye from the previous one or carry insufficient new information. Therefore, we focus on the search for *sufficiently different* explanations (see Section 4.1), which is also our quality metric.

In view of these theoretical results and observations, we present MULTIREX, an approximation algorithm and tool for computing multiple explanations for black box image classifiers. Using the formal mathematical theory of actual causality, MULTIREX computes a causal ranking of the pixels of the image. This ranking is used to construct a refined search landscape (Figure 5), which MULTIREX explores in order to generate multiple, different, explanations. For instance, for the image in Figure 1, MULTIREX finds 4 disjoint explanations where ‘peacock’ is the top classification, whereas altered SAG produces only 1 under the same constraints.

In Section 5 we experimentally compare MULTIREX with altered SAG and with DEEPCOVER Chockler et al. (2021) on standard benchmarks. The results demonstrate that MULTIREX outperforms SAG by the factor of $8.5\times$ wrt the number of completely disjoint explanations it produces. Moreover, MULTIREX produces output on 100% of images, compared to only 20% for SAG, and is $17\times$

faster than DEEPCOVER (Appendix F). We provide the details of the benchmark sets, the models, and the main results in the paper. Results for the original version of SAG are reported in the appendix. The tool, all datasets, and the full set of results are submitted as the supplementary material.

2 Related Work

There is a large body of work on algorithms for computing one explanation for a given output of an image classifier. They can be largely grouped into whitebox and blackbox methods. Whitebox methods frequently use variations on propagation-based explanation methods to back-propagate a model’s decision to the input layer to determine the weight of each input feature for the decision Springenberg et al. (2015); Sundararajan et al. (2017); Bach et al. (2015); Shrikumar et al. (2017); Nam et al. (2020). GRAD-CAM, a whitebox technique which has spawned many variants, only needs one backward pass and propagates the class-specific gradient into the final convolutional layer of a DNN to coarsely highlight important regions of an input image Selvaraju et al. (2017).

Perturbation-based explanation approaches introduce perturbations to the input space directly in search for an explanation. These are typically found in blackbox explanation methods. SHAP (SHapley Additive exPlanations) computes Shapley values of different parts of the input and uses them to rank the features of the input according to their importance Lundberg & Lee (2017). LIME constructs a small neural network to label the original input and its neighborhood of perturbed images and uses this network to estimate the importance of different parts of the input Ribeiro et al. (2016); Datta et al. (2016); Chen et al. (2018); Petsiuk et al. (2018); Fong et al. (2019). Finally, DEEPCOVER ranks elements of the image according to their importance for the classification and uses this ranking to greedily construct a small explanation. The DEEPCOVER ranking procedure Chockler et al. (2021) is based on an approximate computation of causal responsibility. None of these black box tools provide multiple explanations of the same image.

Work on calculating more than one explanation for a given classification outcome is in its infancy. To the best of our knowledge, there is only one algorithm and tool that computes multiple explanations of image classifiers – SAG, described in Shitole et al. (2021). The motivation for SAG is the same as ours: increasing human confidence and trust as well as our understanding of image classification algorithms. We describe SAG’s algorithm in more detail in Section 5 and argue that its definition of explanation is too permissive. Moreover, our experimental results with a standard, strict, definition of explanation outperform SAG by at least an order of magnitude.

For completeness, we also mention a growing body of work on logic-based explanations Ignatiev et al. (2019); Marques-Silva & Ignatiev (2022); Darwiche & Hirth (2023). While the motivation is similar to our work, the problem formulation is very different, as this direction considers the NN as a white-box and attempts to represent it as a logical formula, which is used to derive

explanations about its result. In contrast, our approach is black box and is agnostic to the internal structure of the classifier (nor does it try to represent its decision process as a logic expression).

3 Theoretical Results

In this section we describe the theoretical foundations of our approach and prove worst-case complexity results. We follow the approach by Chockler et al. (2021) (CKS from now on) to defining causes and constructing explanations in image classification. Due to the lack of space, an informal summary of *actual causality* is relegated to Appendix A. The reader is referred to Halpern (2019) for a detailed formal overview and more information on actual causality and responsibility.

We follow the approach of Chockler et al. (2021) (CKS from now on) to defining causes and constructing explanations in image classification. Roughly speaking, we view the NN as a black-box causal model in the Halpern & Pearl (2005)’s-sense of the word, with its inputs being the individual pixels of an input image. The variables are defined as Boolean, with the values being the original color and the masking color¹. For completeness, the relevant definitions and results from CKS are described in Appendix B. Here we only present the definition of explanation for image classification.

Definition 3.1 (Explanation for image classification, CKS). An explanation in image classification is a minimal subset of pixels of a given input image that is sufficient for the NN to classify the image, where “sufficient” is defined as containing only this subset of pixels from the original image, with the other pixels set to the masking color.

A recent paper by Chockler & Halpern 2024 proves that under the same simplifying assumptions that we (and CKS) use, Definition 3.1 is equivalent to the definition of explanation in actual causality Halpern (2019).

CKS observe that the precise computation of an explanation in our setting is intractable, as the problem is equivalent to an earlier definition of explanations in binary causal models, which is DP-complete Eiter & Lukasiewicz (2004) (DP is the class of languages that are an intersection of a language in NP and a language in co-NP and contains, in particular, the languages of unique solutions to NP-complete problems Papadimitriou (1984)). The following lemma shows that computing a second (or any subsequent) explanation is not easier than computing the first one. For the purposes of proving theoretical results, a subsequent explanation is one that differs from the previous ones in at least one pixel; the algorithm in Section 4 constructs spatially different explanations, more suitable to the human perception.

Lemma 3.2. *Given an explanation, constructing a different explanation is DP-complete.*

¹A shown by CKS, a specific masking color does not have almost any effect on the results.

Proof Sketch. Membership in DP is straightforward. For hardness we show a reduction from the problem of computing an explanation. Given an image x classified as $\mathcal{N}(x)$, we construct a *chimera* image from x and an existing explanation of $\mathcal{N}(x)$ (taken from another image) attached to it without obscuring it. Then, our existing explanation is the first explanation to the image being classified as $\mathcal{N}(x)$, and a second one is an explanation of the classification of the original image. \square

We note that the chimera image constructed in the reduction does not have a rectangular shape; however the complexity of the explanation problem does not depend on the shape of the input image.

CKS use a greedy approach to constructing approximate explanations, based on scanning the ranked list of pixels *pixel_ranking*. The pixels are ranked in the order of their *responsibility* for the classification, where responsibility is a quantitative measure of causality and, roughly speaking, measures the amount of causal influence on the classification (see Appendix A for the formal definition). We note, however, that the construction of the ranked list is intractable as well (NP-complete), even in the special case of image classification (Definition B.2), rather than the general definition of responsibility by Chockler & Halpern (2004). Hence, CKS’s ranking is based on the approximate degree of responsibility, which is computed by partitioning the set in iterations and computing the degrees of responsibility for each partition, while discarding low-responsibility elements.

However, reducing the complexity of computing one explanation does not help in reducing the complexity of computing many explanations, as the number of explanations for a given image can be very high, as proven in the following lemma.

Lemma 3.3. *The number of explanations for an input image is bounded from above by $\binom{n}{\lfloor n/2 \rfloor}$, and this bound is tight.*

Proof. Since an explanation of the classification of x is a minimal subset of x that is sufficient to result in the same classification, the number of explanations is characterised by *Sperner’s theorem*, which provides a bound for the number S of largest possible families of finite sets, none of which contain any other sets in the family Anderson (1987). By Sperner’s theorem, $S \leq \binom{n}{\lfloor n/2 \rfloor}$, and the bound is reached when all subsets are of the size $\lfloor n/2 \rfloor$. The following example demonstrates an input on which this bound is reached.

Consider a binary classifier that determines whether an input image of size n has at least $\lfloor n/2 \rfloor$ green-coloured pixels and an input image that is completely green. Then, each explanation is of size $\lfloor n/2 \rfloor$, and there are $\binom{n}{\lfloor n/2 \rfloor}$ explanations. \square

Finally, we note that given a set of explanations (sets of pixels) and an overlap bound, finding a subset of a given number of explanations in which elements overlap for no more than the bound is NP-hard even assuming that constructing and training a binary classifier is $O(1)$ by reduction from the independent set problem, which is known to be NP-complete. Indeed, let \mathcal{N} be a binary classifier

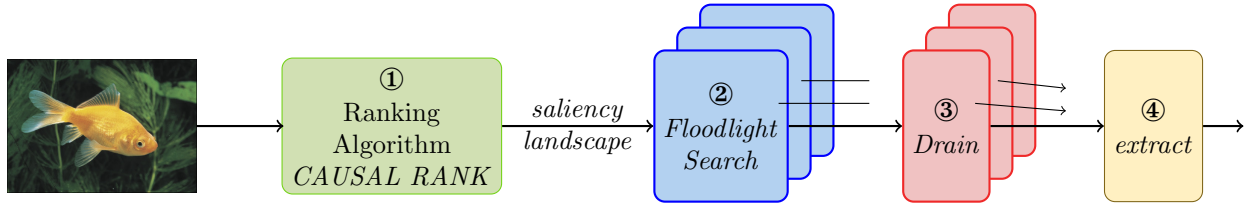


Figure 3: A schematic depiction of our algorithm, returning a set of explanations \mathcal{E} for a given input image. Its components: ① *ranking* generates a saliency landscape of pixels; ② *search* launches x *floodlight* searches over the landscape; ③ *drain* minimizes the explanations found in ②; ④ *extract* produces a maximal subset \mathcal{E} from the output of ③, with the given overlap bound.

that determines whether an input graph $G = \langle V, E \rangle$ contains any connected components of size more than 1. An explanation would be a node $v \in V$ with its adjacent edges. Now, G contains an independent set of size n iff there exist n disjoint explanations of the non-empty label of G given by the classifier, thus proving NP-hardness of the problem.

4 Multiple Explanations

In this section we present our algorithm for computing multiple, different explanations. As shown in Section 3, the problem is intractable, motivating the need for efficient and accurate approximation algorithms. Due to the lack of space, some details and algorithms have been moved to the appendix.

4.1 What is a “Different Explanation”?

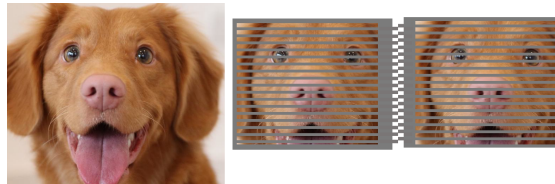


Figure 4: To the human eye, these two explanations for the ‘dog’ label are equivalent, but they do not have any non-background pixels in common. Our spatial approach avoids these problems.

As the goal of constructing different explanations is presenting them to humans for analysis, we need to ensure that the explanations are indeed perceived as different by humans. Consider the explanations in Figure 4. These are obtained

from the original image by dividing it to thin strips horizontally; one explanation then masks all even strips, and the other masks all odd strips. Clearly, the intersection between these explanations is empty. As discussed by Zhang et al. (2015), a human eye fills in the gaps of hazy and low-resolution images. Hence, if we remove a small subset of pixels from a given explanation, it would be sufficiently different from the original one according to many distance measures, yet would likely not be different at all to the human eye (in Figure 4 the gaps are increased for illustrative purposes).

To avoid this problem, we define an *atomic superpixel*, the smallest set of contiguous pixels (a square) that is distinguishable to a human, as a parameter of the algorithm. The concept of a superpixel is used in a number of different explanation tools; SAG splits the image into a fixed grid of 7×7 squares. Dividing the image in this way greatly reduces the computational cost of searching for explanations. The rigidity of the grid, however, leads to missing some explanations. MULTIREX overcomes this problem by generating a random small grid and iteratively refining only the important regions (see Section 5). Furthermore, MULTIREX repeats this procedure with different grids to reduce the influence of particular random choices. The results are combined to produce a detailed saliency landscape Figure 5. The more iterations are added, the smoother and more precise the saliency landscape becomes. We extract explanations from this landscape.

4.2 The MultiReX Algorithm

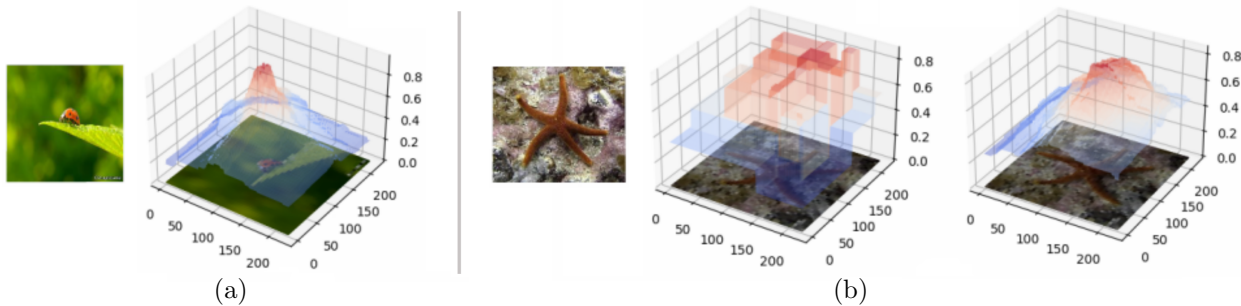


Figure 5: Different saliency landscapes. The image on the left shows shows an image with a single explanation, clearly indicated by the single central peak. The other images show the saliency landscapes of a starfish after 1 and 20 iterations. The landscape here is flatter, with multiple separate peaks. These peaks are likely to correspond with different explanations.

The high-level structure of the algorithm is presented in Figure 3, and the pseudo-code is in Algorithm 1. We discuss each component in more detail below.

The *CAUSAL_RANK* procedure in Line 3 of Algorithm 1 constructs a *pixel_ranking*, which is a ranking of the pixels of the input image x . While any

Algorithm 1 MULTIREX($x, \mathcal{N}, r, n, \delta, p, q$)

INPUT: an image x , a network \mathcal{N} , a floodlight radius r . the maximal number of explanations n , δ maximum overlap between explanations, p number of floodlight expansions, q expansion coefficient

OUTPUT: a set of up to n different explanations \mathcal{E}

```
1:  $\mathcal{E} \leftarrow \emptyset$ 
2:  $l \leftarrow \mathcal{N}(x)$ 
3:  $\mathcal{S} \leftarrow \text{CAUSAL\_RANK}(x, \mathcal{N}, l)$ 
4: for  $i$  in  $0 \dots n - 1$  do
5:    $E_i \leftarrow \text{Floodlight}(x, \mathcal{N}, l, \mathcal{S}, r, n, p, q)$ 
6:    $E_i \leftarrow \text{drain}(x, E_i, \mathcal{N}, \mathcal{S})$ 
7:    $\mathcal{E} \leftarrow \mathcal{E} \cup E_i$ 
8: end for
9:  $\mathcal{E} \leftarrow \text{extract}(\mathcal{E}, \delta)$ 
10: return  $\mathcal{E}$ 
```

pixel ranking mechanism can be used (e.g., an SFL-based ranking in Sun et al. (2020) or LIME or SHAP heatmaps), the quality and the granularity of the final results depend on the quality and the granularity of the ranking. We implemented and tested MULTIREX with causal responsibility-based ranking described in CKS. The number of required explanations is given as an input parameter to the procedure, as the total number of explanations can be exponential (see Lemma 3.3).

The *Floodlight* procedure called in Line 1 is described in Algorithm 2. It replaces the greedy explanation generation in DEEPCOVER with a spatially delimited stochastic hill climb. In contrast to most hill-climb-based algorithms that look for the global maximum, we search for *local maxima*, as these are likely to correspond to explanations. The global maximum usually matches the explanation computed by DEEPCOVER, though it is not guaranteed. The function *initialize* in Line 2 creates a floodlight of radius r at a random position over the image x . We call the model on this masked image. If the initial size of the floodlight, \mathcal{F} , is too small to encompass an explanation, before taking a random step, \mathcal{F} expands in position a fixed number of times. If this increased flooding still does not result in an explanation, the floodlight takes a random step, returning to its original radius. This random step is mediated by an objective function. By default, MULTIREX uses the mean of the responsibility of the pixels under the floodlight. This means the floodlight will tend to move into areas with a higher average responsibility; areas which are more likely to contain an explanation.

Once an explanation is found, MULTIREX performs a local ablation *drain* (see the appendix for details).

Finally, the *extract* procedure (Algorithm 3), extracts a subset of at most n explanations that pairwise overlap up to the input bound δ . As discussed

Algorithm 2 *Floodlight* ($x, \mathcal{N}, l, \mathcal{S}, r, n, p, q$)

INPUT: an image x , a network \mathcal{N} , a label l , a saliency landscape \mathcal{S} , a floodlight radius r , number of steps n , number of expansions p , radius increase q
OUTPUT: an explanation E

```
1:  $\mathcal{F} \leftarrow \text{initialize}(r)$ 
2:  $\mathcal{E} \leftarrow \emptyset$ 
3: for  $i$  in  $0 \dots n - 1$  do
4:   for  $j$  in  $0 \dots p - 1$  do
5:      $l' \leftarrow \mathcal{N}(\mathcal{F}(x))$ 
6:     if  $l = l'$  then
7:        $E \leftarrow \mathcal{F}(x)$ 
8:       return  $E$ 
9:     else
10:       $\mathcal{F} \leftarrow \text{expand\_radius}(r * q)$ 
11:    end if
12:  end for
13:   $\mathcal{F} \leftarrow \text{neighbor}$ 
14: end for
15: return  $E$ 
```

in Section 3, the exact solution is NP-hard. The procedure uses a greedy heuristic based on the Sørensen–Dice coefficient (SDC) Dice (1945); Sørensen (1948), typically used as a measure of similarity between samples. First, we calculate the matrix SDC for all pairs of explanations: $SDC(i, j) = 0$ iff $SDC(E_i, E_j) \leq \delta$, and is $SDC(E_i, E_j)$ otherwise². Columns that sum to 0 correspond to explanations that do not overlap others in more than δ , and are hence added to \mathcal{E} . We then greedily remove the most overlapping explanations and recalculate the overlap matrix, adding the columns summing to 0 to \mathcal{E} . The procedure iterates until SDC is empty.

5 Experimental Results

Implementation We implemented Algorithm 1 in the tool MULTIREX for generating multiple explanations. Given a saliency landscape, by default, MULTIREX attempts to find 10 explanations. While it is computationally relatively inexpensive to search for more explanations than this, on our dataset we observe that images with more than 6 sufficiently different explanations are extremely rare ($\approx 1\%$ of images). The algorithm computes multiple maximally different approximations of causal explanations according to Definition 3.1.

²For disjoint explanations, i.e., $\delta = 0$, we can simply take $E_i \cap E_j$ instead of $SDC(i, j)$.

Algorithm 3 *extract*(\mathcal{E}, δ)

INPUT: a set of explanations \mathcal{E} , a permitted degree of overlap δ
OUTPUT: a subset of explanations $\mathcal{E}' \subseteq \mathcal{E}$ with overlap at most δ

```
1: all_pairs  $\leftarrow \mathcal{E} \times \mathcal{E}$ 
2:  $m \leftarrow 0_{|\mathcal{E}|, |\mathcal{E}|}$ 
3: for  $(p_i, p_j)$  in all_pairs do
4:    $SDC \leftarrow dice\_coefficient(p_i, p_j)$ 
5:    $m_{p_i, p_j} = SDC > \delta ? SDC : 0$ 
6: end for
7:  $\mathcal{E}' \leftarrow \emptyset$ 
8: for  $i$  in  $0 \dots |\mathcal{E}| - 1$  do
9:   for  $j$  in  $0 \dots cols(m)$  do
10:    if  $sum(col_j) = 0$  then
11:       $\mathcal{E}' \leftarrow \mathcal{E}' \cup \mathcal{E}_j$ 
12:    end if
13:  end for
14:   $m \leftarrow remove\_most\_overlapping\_explanation(m)$ 
15: end for
16: return  $\mathcal{E}'$ 
```

Modifications to Sag As discussed earlier, SAG partitions the input image into a fixed 7×7 grid. SAG accepts a region as an explanation if the confidence of the original label on this region is greater than a confidence bound. The confidence bound of SAG is based on a hyperparameter ‘probability threshold’ and the confidence of the model on the original image. This is regardless of the position of this label in the total softmax output. This in contrast with MULTIREX’s stricter definition of explanation, which, similarly to other explainability tools such as LIME and SHAP, only considers explanations with the top label matching the label of the whole image. We illustrate the importance of this difference in Figure 6, where a region of the original image labeled ‘peacock’ is output as an explanation for the label by SAG, even though this region’s top label is actually ‘monitor’, and ‘peacock’ is only the 12th (note also that SAG reports 67% confidence in this explanation, which is misleading, as it does not correspond to any meaningful measure of confidence in the label). To enable a direct comparison of the results, we alter SAG slightly (changing 4 lines of code) so that it only outputs explanations with the top label matching the label of the original image. We denote this version A-SAG and we compare MULTIREX with it. As MULTIREX does not impose a confidence bound on explanations, our experimental results are on A-SAG with the probability threshold lowered to 0.4 and 0.1 (the original SAG’s threshold is 0.9), making the results more favorable to A-SAG. We present the comparison with the original SAG in Appendix E.

Explanations are presented in the form of a directed acyclic graph, or



Figure 6: SAG’s explanation for ‘peacock’ (Figure 1a) with 0.4 probability threshold. VGG19’s top classification for this image is ‘monitor’, with ‘peacock’ only in 12th position.

Structured Attention Graph (SAG). Multiple explanation diversity is enforced by bounding the maximal overlap in terms of a number of regions shared between explanations. SAG addresses the exponential number of candidates (2^{49}) by randomly selecting subsets.

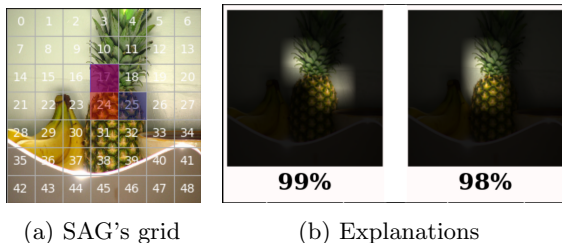


Figure 7: Two explanations from SAG overlapping on the square no.17. SAG has a rigid overlap size (one square on the grid). MULTIREX’s overlap is a parameter and depends on the size of both explanations.

Hyperparameters Both tools offer a number of tunable hyperparameters. SAG has 9 tunable hyperparameters, all of which can potentially affect the output, often in unpredictable ways; MULTIREX has 7 hyperparameters, whose effect on the output is limited to the overlap between explanations (see Table 3 in the appendix). We set both tools to 10 as the maximum number of explanations. SAG requires the user to set the maximal allowed overlap in grid squares, with suggested values of 0, 1, or 2. MULTIREX does not measure overlap in blocks, as it is not tied to a fixed grid. For a fair comparison, we filter MULTIREX explanations to be non-overlapping, using the SDC coefficient, and limit SAG to non-overlapping explanations as well. Apart from the changes discussed above, the experiments are performed on MULTIREX and both versions of SAG with default settings.

Datasets and Models For our experiments, we used the standard dataset of ImageNet-mini³, consisting of 3923 images representing 1000 different labels. SAG uses the pytorch VGG19 model by default. To enable a fairer comparison, we used the onnx⁴ version of VGG19 for MULTIREX⁵.

Our explanations explain the model’s classification and their quality inherently depends on the model’s quality. Hence, we do not include out-of-distribution images in our dataset.

Experimental Results A natural performance measure for multiple explanations is the number of multiple significantly different explanations produced for each image. We tested SAG and MULTIREX with the option of producing completely disjoint explanations. MULTIREX can accept any degree of overlap between explanations, whereas SAG is limited by its grid. Searching for explanations with no overlap at all provides the fairest and the easiest comparison.

The main experiment was performed on a 64-core machine running Ubuntu 20.04.6 with a 48GB RAM Nvidia A40 GPU. We set a timeout (TO) of 10 minutes for each tool on each image.

Figure 8 shows the breakdown of the results by to the number of images having a particular number of disjoint explanations found by MULTIREX and by SAG, respectively. The results are also presented in the tabular form in Table 1. The most notable result, apart from explanation multiplicity, is the fact that A-SAG does not provide any explanation at all for $\approx 80\%$ of images. This is due to the exhaustion of the search budget over the rigid, predefined, grid. MULTIREX does not suffer from this problem, as it uses causal ranking to build a search landscape not bound to any particular grid. In general, the worst case output for MULTIREX is the whole image returned as the (single) explanation, and hence MULTIREX always succeeds, unlike the random, limited, attempts of SAG. As a superpixel in SAG has a fixed size, $1/49^{th}$ of the input image, it can result in very similar, though not overlapping, explanations if the explanations are small (see an illustration in Figure 7). We also present the results of a small experiment on partially occluded images in Appendix D, indicating that MULTIREX successfully finds non-contiguous explanations, whereas SAG does not.

SAG’s performance is strongly tied to the exact value of its probability threshold. Even when we fix SAG to consider only the top results, the probability threshold still filters out many explanations where they were the top explanation from the model. For example, A-SAG at 0.1 finds 8 images with 10 explanations, compared to just 2 for A-SAG at 0.4. These extra explanations still indicate the best result from the model, but may be missed by a poor settings of the probability threshold. We conjecture that these low confidence predictions are more likely to contain misclassifications.

³<https://www.kaggle.com/datasets/iftgotin/imagenetmini-1000>

⁴<https://onnxruntime.ai/>

⁵<https://github.com/onnx/models>

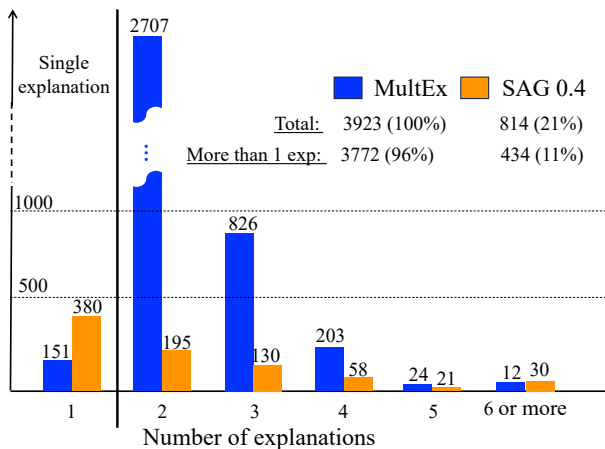


Figure 8: Number of disjoint explanations found by SAG and MULTIREX on Imagenet-mini dataset (The fewer images with 1 explanation, the better).

Timings MULTIREX takes an average of 23s per image on our machine, for 20 iterations of the main algorithm. Original SAG, with the default probability threshold 0.9, takes an average of 26s. Reducing the probability threshold leads to faster execution of SAG ($\approx 15s$), however introduces explanations of decreased quality (see Figure 6). A-SAG is faster, due to the quick exhaustion of the search budget. A-SAG, with probability threshold 0.4, takes an average of 10s to complete, though it only completes for approximately 21% of images (Table 1). We also executed both MULTIREX and original SAG (at 0.9) on a machine without GPU support, an AWS instance using a cluster of Inter Xeon Platinum 8375D CPU @ 2.90 GHz. MULTIREX finished on all images within the TO budget, whereas SAG only finished on $\approx 49\%$ of the images.

6 Conclusions and Future Work

Motivated by studies in human cognition and the need for thorough debugging of image classifiers, this paper proposes an algorithm and a tool MULTIREX for constructing multiple explanations for the outputs of image classifiers. The algorithm is based on the solid mathematical foundations of causal reasoning and is agnostic to the classifier, viewing it as a black box. The tool MULTIREX is modular and consists of two main building blocks: the ranking procedure and the explanation-discovery procedure. We introduce a novel explanation-discovery algorithm based on the saliency landscape constructed in the ranking procedure and a “floodlight” search, ensuring different spatial locations for explanations and avoiding the problem of different, but visually similar explanations.

MULTIREX finds multiple different explanations of image labels on standard benchmark sets and is fully configurable. Moreover, by default MULTIREX does

No. Explanations	Tools		
	MULTIREX	A-SAG 0.4	A-SAG 0.1
1	151	380	448
2	2707	195	166
3	826	130	107
4	203	58	42
5	24	21	19
6	7	15	14
7	2	8	8
8	2	3	3
9	1	2	2
10	0	2	8
Total (%)	100%	21%	20%

Table 1: Number of disjoint explanations produced by MULTIREX against A-SAG. A-SAG completes on $\approx 20\%$ of the images, even with the confidence scalar lowered to 0.1.

not depend on the probabilities assigned to the labels by the classifier. We compare our experimental results with SAG, the only other tool for multiple explanations, and demonstrate that MULTIREX finds multiple explanations on 96% of images, whereas SAG, slightly modified to allow comparison, finds them only on 11% of images. Moreover, MULTIREX terminates on the whole benchmark set, in contrast to the altered version of SAG that fails to complete on 80% of it. For completeness, we compared the performance of MULTIREX with the state-of-the-art tool DEEPCOVER, demonstrating $17\times$ speedup (see Appendix F).

There is a number of promising directions for future work. We have seen that different methods for extracting explanations from the landscape produce explanations of different sizes; this needs further investigation. Furthermore, we hypothesise that the precision of ranking drops for the lower ranked elements, affecting the quality of explanations that are lower on the saliency landscape. While the intractability of computing an exact explanation implies a tradeoff between the quality of the approximation and the precision of the result, we will search for new heuristics to improve the quality of the saliency landscape at low levels.

References

- Anderson, I. *Combinatorics of Finite Sets*. Oxford University Press, 1987.
- Bach, S., Binder, A., Montavon, G., Klauschen, F., Müller, K.-R., and Samek,

- W. On pixel-wise explanations for non-linear classifier decisions by layer-wise relevance propagation. *PLOS One*, 10(7), 2015.
- Chen, J., Song, L., Wainwright, M., and Jordan, M. Learning to explain: An information-theoretic perspective on model interpretation. In *International Conference on Machine Learning (ICML)*, volume 80, pp. 882–891. PMLR, 2018.
- Chockler, H. and Halpern, J. Y. Responsibility and blame: A structural-model approach. *J. Artif. Intell. Res.*, 22:93–115, 2004.
- Chockler, H. and Halpern, J. Y. Explaining image classifiers, 2024.
- Chockler, H., Kroening, D., and Sun, Y. Explanations for occluded images. In *IEEE/CVF International Conference on Computer Vision, ICCV*, pp. 1214–1223. IEEE, 2021.
- Darwiche, A. and Hirth, A. On the (complete) reasons behind decisions. *J. Log. Lang. Inf.*, 32(1):63–88, 2023.
- Datta, A., Sen, S., and Zick, Y. Algorithmic transparency via quantitative input influence: Theory and experiments with learning systems. In *Security and Privacy (S&P)*, pp. 598–617. IEEE, 2016.
- Dice, L. R. Measures of the amount of ecologic association between species. *Ecology*, 26:297—302, 1945.
- Eiter, T. and Lukasiewicz, T. Complexity results for explanations in the structural-model approach. *Artif. Intell.*, 154(1-2):145–198, 2004.
- Fan, S., Koenig, B. L., Zhao, Q., and Kankanhalli, M. S. A deeper look at human visual perception of images. *SN Computer Science*, 1(58), 2020.
- Fong, R., Patrick, M., and Vedaldi, A. Understanding deep networks via extremal perturbations and smooth masks. In *International Conference on Computer Vision (ICCV)*, pp. 2950–2958. IEEE, 2019.
- Halpern, J. Y. A modification of the Halpern–Pearl definition of causality. In *Proceedings of IJCAI*, pp. 3022–3033. AAAI Press, 2015.
- Halpern, J. Y. *Actual Causality*. The MIT Press, 2019.
- Halpern, J. Y. and Pearl, J. Causes and explanations: A structural-model approach. Part I: Causes. *British Journal for the Philosophy of Science*, 56(4), 2005.
- Hanson, N. R. *Patterns of Discovery: An Inquiry into the Conceptual Foundations of Science*. Cambridge University Press, 2010.
- Hume, D. *A Treatise of Human Nature*. John Noon, 1739.

- Ignatiev, A., Narodytska, N., and Marques-Silva, J. Abduction-based explanations for machine learning models. In *The Thirty-Third AAAI Conference on Artificial Intelligence, AAAI*, pp. 1511–1519. AAAI Press, 2019.
- Lin, T.-Y., Maire, M., Belongie, S., Hays, J., Perona, P., Ramanan, D., Dollár, P., and Zitnick, C. L. Microsoft COCO: Common objects in context. In *European conference on computer vision*, pp. 740–755. Springer, 2014.
- Lundberg, S. M. and Lee, S.-I. A unified approach to interpreting model predictions. In *Advances in Neural Information Processing Systems (NeurIPS)*, volume 30, pp. 4765–4774, 2017.
- Marques-Silva, J. and Ignatiev, A. Delivering trustworthy AI through formal XAI. In *Thirty-Sixth AAAI Conference on Artificial Intelligence, AAAI*, pp. 12342–12350. AAAI Press, 2022.
- Miller, T. Explanation in artificial intelligence: Insights from the social sciences. *Artificial Intelligence*, 267:1–38, 2019.
- Nam, W.-J., Gur, S., Choi, J., Wolf, L., and Lee, S.-W. Relative attributing propagation: Interpreting the comparative contributions of individual units in deep neural networks. In *AAAI Conference on Artificial Intelligence*, volume 34, pp. 2501–2508, 2020.
- Papadimitriou, C. The complexity of unique solutions. *Journal of ACM*, 31: 492–500, 1984.
- Petsiuk, V., Das, A., and Saenko, K. RISE: randomized input sampling for explanation of black-box models. In *British Machine Vision Conference (BMVC)*. BMVA Press, 2018.
- Ribeiro, M. T., Singh, S., and Guestrin, C. “Why should I trust you?” Explaining the predictions of any classifier. In *Knowledge Discovery and Data Mining (KDD)*, pp. 1135–1144. ACM, 2016.
- Selvaraju, R. R., Cogswell, M., Das, A., Vedantam, R., Parikh, D., and Batra, D. Grad-CAM: Visual explanations from deep networks via gradient-based localization. In *International Conference on Computer Vision (ICCV)*, pp. 618–626. IEEE, 2017.
- Shitole, V., Li, F., Kahng, M., Tadepalli, P., and Fern, A. One explanation is not enough: Structured attention graphs for image classification. In *Neural Information Processing Systems (NeurIPS)*, pp. 11352–11363, 2021.
- Shrikumar, A., Greenside, P., and Kundaje, A. Learning important features through propagating activation differences. In *International Conference on Machine Learning (ICML)*, volume 70, pp. 3145–3153. PMLR, 2017.

- Sørensen, T. A method of establishing groups of equal amplitude in plant sociology based on similarity of species and its application to analyses of the vegetation on Danish commons. *Kongelige Danske Videnskabernes Selskab.*, 5: 1—34, 1948.
- Springenberg, J. T., Dosovitskiy, A., Brox, T., and Riedmiller, M. A. Striving for simplicity: The all convolutional net. In *ICLR (Workshop Track)*, 2015. URL <http://arxiv.org/abs/1412.6806>.
- Sun, Y., Chockler, H., Huang, X., and Kroening, D. Explaining image classifiers using statistical fault localization. In *ECCV, Part XXVIII*, volume 12373 of *LNCS*, pp. 391–406. Springer, 2020.
- Sundararajan, M., Taly, A., and Yan, Q. Axiomatic attribution for deep networks. In *International Conference on Machine Learning*, pp. 3319–3328. PMLR, 2017.
- van Dyck, L. E., Kwitt, R., Denzler, S. J., and Gruber, W. R. A deeper look at human visual perception of images. *Front. Neurosci.*, 15, 2021.
- Zhang, X.-S., Gao, S.-B., Li, C.-Y., and Li, Y.-J. A retina inspired model for enhancing visibility of hazy images. *Front. Comput. Neurosci.*, 9, 2015.

A Background on Actual Causality

Our definitions are based on the framework of *actual causality* introduced by Halpern & Pearl (2005). The reader is referred to that paper and to Halpern (2019) for an updated overview and more information on actual causality. Due to the lack of space, we omit formal definitions and instead discuss the intuition informally. This is sufficient for our purposes, as we explain below.

The definition of an *actual cause* is based on the concept of *causal models*, which consist of a set of variables, a range of each variable, and structural equations describing the dependencies between the variables. Actual causes are defined with respect to a given causal model, a given assignment to the variables of the model (a context), and a propositional logic formula that holds in the model in this context.

Actual causality extends the simple counterfactual reasoning Hume (1739) by considering the effect of *interventions*, which are changes of the current setting. Roughly speaking, a subset of variables X and their values in a given context is an actual cause of a Boolean formula φ being True if there exists a change in the values of other values that creates a counterfactual dependency between the values of X and φ (that is, if we change the values of variables in X , φ would be falsified). The formal definition by Halpern & Pearl (2005) and in its modifications, the latest of which is by Halpern (2015), are far more complex due to the potential dependencies between the variables and considering causes of more than one element. In our setup, where we are only interested in

singleton causes and in interventions only on the input variables, all versions of the definition of (a part of) an actual cause are equivalent to our definition under the assumption of independence between the input variables.

Responsibility, as defined by Chockler & Halpern (2004) and adapted to the modified definition of causality by Halpern (2015), is a quantification of causality, attributing to each actual cause its *degree of responsibility*, which is derived from the size of a smallest contingency required to create a counterfactual dependence. The degree of responsibility is defined as $1/(k + 1)$, where k is the size of a smallest contingency. The degree of responsibility of counterfactual causes is therefore 1 (as $k = 0$), and the degree of responsibility of variables that have no causal influence on φ is 0, as k is taken to be ∞ . In general, the degree of responsibility is always between 0 and 1, with higher values indicating a stronger causal dependence.

B Causes and explanations in image classification

We follow the approach by Chockler et al. (2021) (CKS from now on) to defining causes and constructing explanations in image classification. Roughly speaking, we view the NN as a black-box causal model in the Halpern & Pearl (2005)-sense of the word, with its inputs being the individual pixels of an input image. The variables are defined as Boolean, with the values being the original color and the masking color.⁶ Following Halpern (2019), we further augment the model by limiting the allowed interventions to masking the colors of input’s pixels. Moreover, we are only interested in singleton causes (recall that we assume independence between the input variables).

Definition B.1 (Singleton cause for image classification, CKS). For an image x classified by the NN as $f(x) = o$, a pixel p_i of x is a *cause* of o iff there exists a subset P_j of pixels of x such that the following conditions hold:

- SC1.** $p_i \notin P_j$;
- SC2.** changing the color of any subset $P'_j \subseteq P_j$ to the masking color does not change the classification;
- SC3.** changing the color of P_j and the color of p_i to the masking color changes the classification.

We call such P_j a *witness* to the fact that p_i is a cause of x being classified as o .

Definition B.2 (Simplified responsibility, CKS). The *degree of responsibility* $r(p_i, x, o)$ of p_i for x being classified as o is defined as $1/(k + 1)$, where k is the size of the smallest witness set P_j for p_i . If p_i is not a cause, k is defined as ∞ , and hence $r(p_i, x, o) = 0$. If changing the color of p_i alone to the masking color results in a change in the classification, we have $P_j = \emptyset$, and hence $r(p_i, x, o) = 1$.

⁶A shown by CKS, a specific masking color does not have almost any effect on the results.

Lemma B.3 (CKS). *Definition B.1 is equivalent to the definition of an actual cause when input variables in the model are independent of each other, and we do not consider interventions on internal variables.*

Corollary B.4 (CKS). *The problem of detecting causes in image classification is NP-complete.*

C Algorithm *drain*

Algorithm 4 *drain* ($x, E, l, \mathcal{N}, \mathcal{S}$)

INPUT: an image x , a label l , a network \mathcal{N} , a saliency landscape \mathcal{S}

OUTPUT: an explanation E

- 1: $levels \leftarrow$ all unique causal values, ranked high to low
 - 2: $E \leftarrow$ *binary_search*($\mathcal{N}, levels, l$)
-

Once an explanation is found, MULTIREX performs a local ablation *drain* (see the full version for details), essentially lowering and raising the water level so that only the explanation is above water. This procedure is necessary to minimise the explanation provided by the floodlight. While it would be possible, as per DEEPCOVER, to remove one pixel at a time from the mask, this is computationally extremely expensive. Instead, we take the spatially appropriate part of the pixel ranking and remove all pixels of equal responsibility, until we have the smallest passing mask. To further increase the efficiency of this procedure, we perform it at a modified binary search. We find all unique pixel ranking in the region and order this from high to low. The binary search then proceeds in the usual manner, but setting all pixels from highest to the mid point as true. What we gain in performance can lead to a slight bloating of explanation, especially those explanations which are lower in the responsibility ranking. Due to the nature of causal ranking, those pixels which do not contribute often to an explanation have relatively flat landscapes, as can be seen in Figure 5. An explanation found in a lower lying region of the landscape, therefore, will usually have a flatter terrain, meaning more pixels are introduced into the explanation than required for minimality. One can see an example of this in Figure 2, where the procedure has not completely drained away all background in the third image.

D Occluded Images

As MULTIREX’s explanation extraction algorithm is based on a spatial search Algorithm 2, discovery of non-contiguous explanations can become challenging. We have not conducted a comprehensive study on multiple explanations of partially occluded images. However, a preliminary experiment indicates that MULTIREX



(a) Ocluded bus

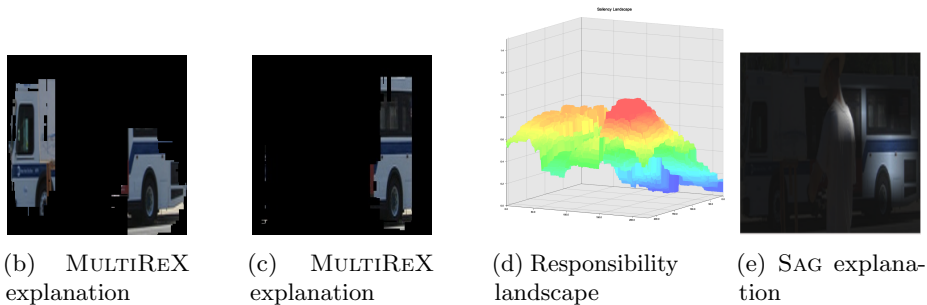


Figure 9: Figure 9b shows a disjoint explanation produced by MULTIREX for Figure 9a. MULTIREX also produces the explanation Figure 9c which contains just a thin strip of the bus on the left hand side. While a smaller explanation, a human might prefer Figure 9b. Figure 9d shows the responsibility landscape MULTIREX produces. All explanations are resized to 224×224 as per model requirements. Figure 9e shows that SAG fails to find a disjoint explanation and included the man’s shoulder.

successfully finds a non-contiguous explanation of a partially occluded image, if supported by the model Figure 9e (the image is taken from Lin et al. (2014)). SAG, in contrast, failed to find a non-contiguous explanation. The same model, VGG19, as in our main experiment, is used for this comparison.

E Comparison with Unaltered Sag

We ran SAG without our alterations as well, for confidence scalars of 0.9, 0.4 and 0.1. As expected, the number of multiple explanations increases as SAG’s leeway increases. It is not until SAG’s confidence scalar is as low as 0.1 that it comprehensively out finds explanations against MULTIREX. For all settings, MULTIREX still finds more multiple explanations in total. The explanations for SAG 0.1 have, essentially, little to no quality check at all attached to them, unlike for MULTIREX, which always considers the highest scoring classification.

No. Exp	Tools			
	MULTIREX	SAG 0.9	SAG 0.4	SAG 0.1
1	151	3243	2476	1532
2	2707	489	816	1012
3	826	123	345	566
4	203	48	155	354
5	24	12	69	193
6	7	4	34	120
7	2	0	19	58
8	2	1	3	31
9	1	0	1	32
10	0	3	0	25
%	100%	100%	100%	100%

Table 2: Number of disjoint explanations produced by MULTIREX against original SAG. Even though SAG has the advantage of searching through the entire model output to match its classification target, MULTIREX still outperforms it or is comparable for most explanation multiplicities.

F Comparison with DeepCover

Both DEEPCOVER and MULTIREX use causal reasoning to rank the pixels of the image. The tools differ in the procedure of extracting explanations. A direct comparison between the two makes little sense, as DEEPCOVER produces only one explanation per image. Instead, we conducted a small-scale experiment on the data contained in the DEEPCOVER GitHub repository. Both DEEPCOVER and MULTIREX were executed for 20 iterations, and we compared their performance. MULTIREX is ≈ 17 times faster than DEEPCOVER.

G Hyperparameters

Both tools have a number of hyperparameters, as shown in Table 3. MULTIREX in particular inherits a number of parameters from DEEPCOVER which do not affect the performance *wrt* multiple explanations. For MULTIREX we left everything at default value. We did not conduct any large investigation into the effect of varying the hyperparameter values. Both tools have other parameters which are not directly editable by the user. We do not include these in the hyperparameter count. MULTIREX’s hyperparameters, with the exception of “spotlights”, do not directly affect the number of explanations found. MULTIREX will always return the number of explanations equal to the value of “spotlights”. The other values, however, may have an effect on how many non-overlapping explanations are found, as they put bounds on the search time of the floodlight

SAG	MULTIREX
ups	iters
prob_thresh	min_size
numCategories	spotlights
node_prob_thresh	spotlight_size
beam_width	spotlight_eta
max_num_roots	obj_function
overlap_thresh	mask_value
numSuccessors	
num_roots_sag	

Table 3: Hyperparameters for SAG and MULTIREX

algorithm.